PROCEEDINGS OF SCIENCE

Combining Hough Transform and Optimal Filtering for Efficient Cosmic Ray Detection with a Hadronic Calorimeter

Luciano M. de A. Filho[*†]
Federal University of Rio de Janeiro
E-mail: lucianom@lps.ufrj.br

José M. de Seixas
Federal University of Rio de Janeiro
E-mail: seixas@lps.ufrj.br

The hadronic calorimeter of ATLAS, TileCal, provides a large amount of readout channels (about 10,000). Therefore, track detection may be performed by TileCal when cosmic muons cross the detector. The muon track detection has extensively been used in the TileCal commissioning phase, for both energy and timing calibrations, and it will also be important for background noise removal during nominal LHC operation. This work presents a cosmic ray detection algorithm based on TileCal information. The algorithm employs the Hough Transform to map the data from activated calorimeter cells into a parameter (straight-line track) space, in which detection is effectively performed. Due to intrinsic low signal-to-noise ratio for cosmic ray detection with TileCal, a preprocessing algorithm based on a matched filter operating over TileCal time sampled signals is implemented to improve detection efficiency. Experimental data shows that the proposed method possesses extensive efficiency superiority over straight-line fitting produced by least-square methods.

XII Advanced Computing and Analysis Techniques in Physics Research
November 3-7 2008
Erice, Italy

[*]Speaker.
[†]This work was supported by CNPq, FAPERJ and CAPES (Brazilian national research funding agencies).

1. Introduction

ATLAS detector [1] is at final phase of a detailed test and calibration process. For that, tests using Cosmic Rays (CR) as source is being performed in different sub-detectors. An important task in this stage is the measurement of the deposited energy, left by a CR when it crosses the calorimeter. In order to evaluate this task, an efficient track detection algorithm, looking at the activated calorimeter cells, should be implemented. In this way, one can check the reconstructed data coherency, look for potential problems and test the calorimeter energy uniformity.

The previous cosmic ray detection algorithm used in the hadronic calorimeter (TileCal) seeks to minimize the summing of quadratic distances among activated cells and the desired tracks [2], using Least Square Methods (LSM). However, the LSM has an inherent limitation: the sensibility to outliers [3]. In other words, although LSM manipulates measurement errors which appears as small fluctuation in the data set efficiently, it does not tolerate outliers. This kind of noise, even in small quantity, produce residues, generating wrong track adjustments. Besides, the LSM is not able to detect multiple tracks itself.

This work presents an alternative cosmic ray detection algorithm in TileCal, using the Hough Transform (HT) method [4]. This techniques is extensively used to detect line segments in highly noisy images and was here adapted to detect tri-dimensional tracks. HT proved to be able to deal with the noise contamination present in cosmic ray track detection procedure in TileCal and has shown to be an useful method to detect multiple tracks in a more direct way.

Due to the low signal-to-noise ratio of TileCal for cosmic rays, we have shown that matched-filters [5], operating over the time sampled signals of individual calorimeter cells, give higher signal detection efficiency than standard energy cut procedures. This reduces the number of outlier, increasing the muon track detection algorithm efficiency.

The combination of Hough Transform and Matched-Filter techniques has shown to be an efficient approach to detect cosmic rays in ATLAS hadronic calorimeter. The implemented methods and some important analysis results are presented.

2. The ATLAS detector

As one of the main LHC [6] detectors, ATLAS will explore the fundamental nature of matter and the basic forces that shape our universe. The detector has a total length of 42 m and a radius of 11 m (see Figure 1).

The Inner Detector [7] extends to a radius of 1.2 m, and is 7 m in length along the beam pipe. Its basic function is to track charged particles, revealing detailed information about the type of particle and its momentum. The calorimeter [8] is situated outside the solenoidal magnet that surrounds the inner detector and comprises two sections: an electromagnetic [9] and a hadronic [10] part. Their purpose is to measure the energy of incoming particles by total absorption [11]. The muon spectrometer is an extremely large detection system, extending from a radius of 4.25 m around the calorimeters out to the full radius of the detector (11 m) [12]. Its tremendous size is required to accurately measure the momentum of muons.

Due to the extremely high interaction rate and the huge background noise generated by LHC, ATLAS requires the design of a sophisticated on-line triggering system, for which calorimeters

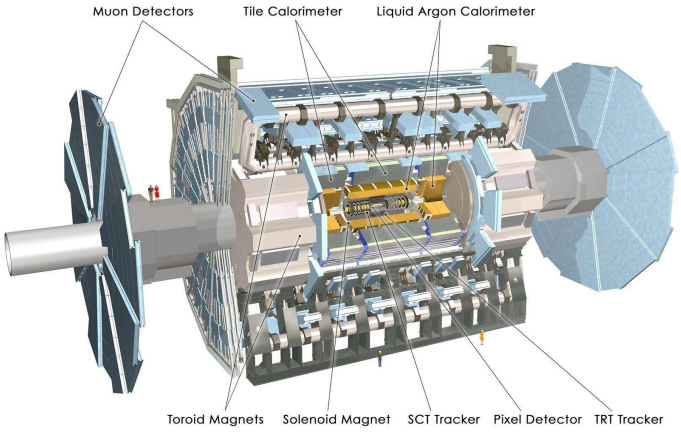

Figure 1: The ATLAS and its main subsystems (extracted from [1]).

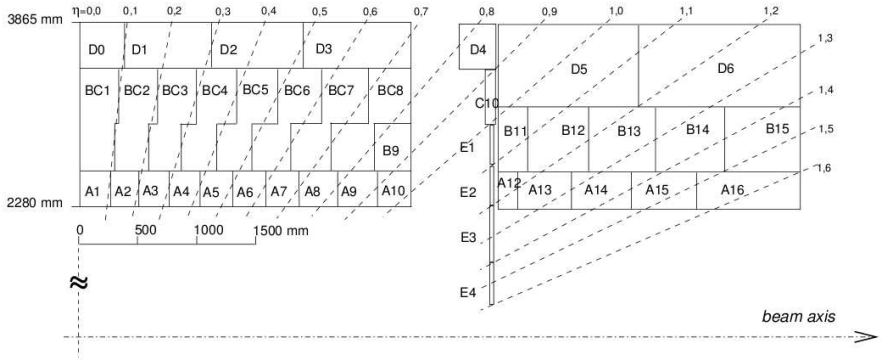

Figure 2: TileCal segmentation (extracted from [1]).

provide an essential information. In ATLAS, the triggering system operation is split into three cascaded levels and should reduce dramatically the background noise rate, providing an output frequency of the order of 100 Hz [13].

2.1 TileCal segmentation

The TileCal absorbs energy from particles that pass through the EM calorimeter, these particles are primarily hadrons. The energy-absorbing material is steel and scintillating tiles sample the deposited energy.

The TileCal comprises three cylindrical parts: one barrel, which covers the rapidity range $|\eta| < 1.0$ (in ATLAS coordinates [1]), and two extended barrel wheels, covering the rapidity range $0.8 < |\eta| < 1.7$ on either side of the barrel. The barrel and the two extended barrels are separated by a gap of 600 *mm* to provide space for liquid argon distribution pipes. Each of the sub-detectors is composed of 64 azimuthal wedge-shaped modules. Figure 2 shows the TileCal segmentation. Each Calorimeter cell is coupled to two PMTs for readout redundancy.

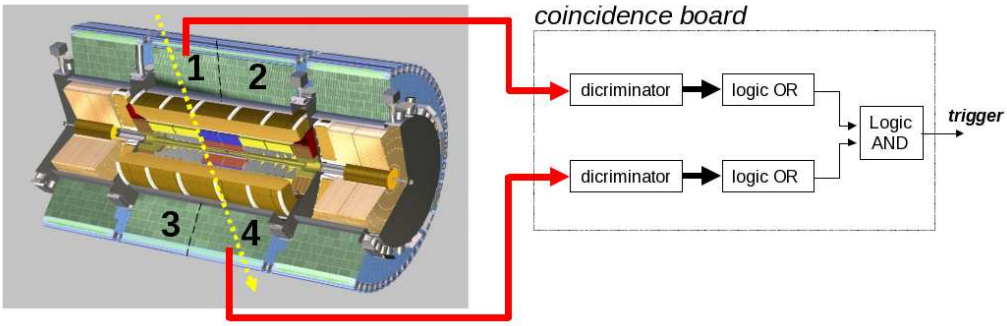

Figure 3: Triggering cosmic rays with TileCal.

3. Commissioning with cosmic rays

The goal of the calorimeter commissioning with cosmic rays [14] is the performance validation of the calibrated detector, ensuring the readiness for LHC turn-on. In order to acquire cosmic data, the ATLAS trigger system is bypassed and a coincidence board assembled for this proposal [15] is used. Figure 3 shows how the setup works. The straight-line represents a cosmic muon crossing the center of the detector. For triggering, coincidence from both top and bottom parts of the TileCal is required. When a trigger signal is generated, data from both hadronic and electromagnetic calorimeters can be recorded with total granularity. The coincidence board uses compacted information from TileCal, obtained from its trigger towers. These towers correspond to the analog sum of all PMTs inside $\Delta\eta < 0.1$, for each module. In Figure 2, one can identify, for instance, that the first tower corresponds to the sum of signals from A1, BC1 and D0 cells.

Cosmic ray muons can be used to check various detector parameters. While the cell by cell statistics might not be sufficient, it will be possible to sum similar cells (along the ϕ direction) and perform physics signal shape studies, as well as amplitude and time inter-calibrations. The problematic channels, such as having HV different from nominal voltage, dead readout channels etc, can be identified, and proper treatment of these channels can be investigated.

4. Cosmic ray detection algorithms

In order to detect cosmic rays in TileCal, two different techniques were combined. The track detection itself is done using Hough Transform (HT) methods. To identify which calorimeter cells will be used by the HT algorithms (candidate cells having energy deposition), a signal detection using matched-filters is performed, looking at the digital samples of individual cells.

4.1 Track detection with Hough Transform

Hough Transform (HT) is a well known technique for image processing aiming at detecting straight lines in noisy and missing information environments [16]. HT maps $\Re^2$ in a parameter space of either linear or sinusoidal functions. When the mapping functions is

$$\rho = x\cos\theta + y\sin\theta \tag{4.1}$$

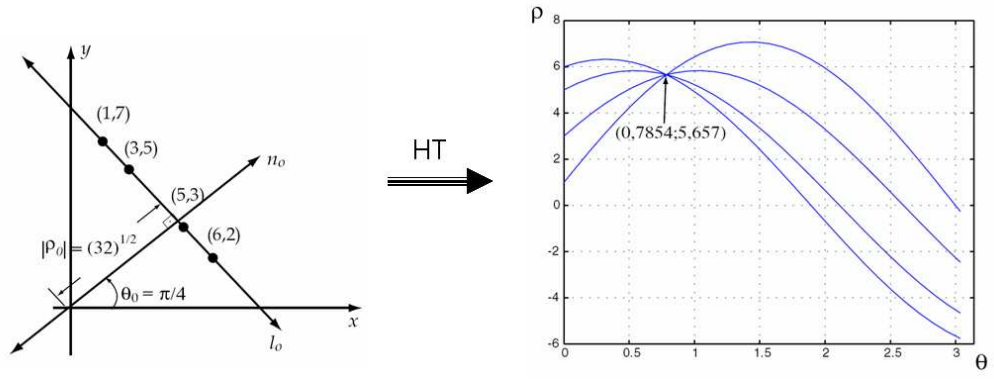

Figure 4: Hough Transform applied to points which belong to the same line.

all data points in the *x*-*y* plane located on the line $\rho_0 = x\cos\theta_0 + y\sin\theta_0$ are mapped onto curves in the ρ-θ Hough space (see Figure 4), with all curves passing trough (ρ_0, θ_0).

To evaluate the algorithm, both ρ and θ axes have to be quantized and hence a two-dimensional accumulator array be constructed in the ρ-θ plane. The HT equation is applied to each point in the data set and contents of all the cells in the transform plane that the corresponding curve passes trough are incremented. Then, a search is performed to locate a number of maximal bins in the ρ-θ plane.

The HT approach as presented above has an extensive computational cost since the coordinates ρ and θ need to be quantized finely in most of the practical applications. Some variations of the standard HT method were proposed in order to reduce the computational cost. Among them, the Local Hough Transform (LHT) [17] and the Adaptive Hough Transform (AHT) [18] are used in this work.

4.1.1 Implementation in TileCal

In order to implement a cosmic ray track detection in TileCal using HT, some steps should be executed before to perform the track detection itself. The whole procedure is listed bellow:

1. Select only activated cells, either applying energy cuts or using matched filters for signal detection.
2. Replace cell geometry by theirs (x,y,z) center point position.
3. Project center points of activated cells in two orthogonal planes. XY and ZY planes were used.
4. Find straight lines in each plane using the HT method.
5. Merge the line segments from each plane in 3D tracks.

The implemented HT algorithm was a combination of LHT with two AHT iterations. Cell energy information is used as weight in the second iteration in order to get thinner track adjustments. Figure 5 shows an example of cosmic ray detection in TileCal using HT. A fit method is shown for

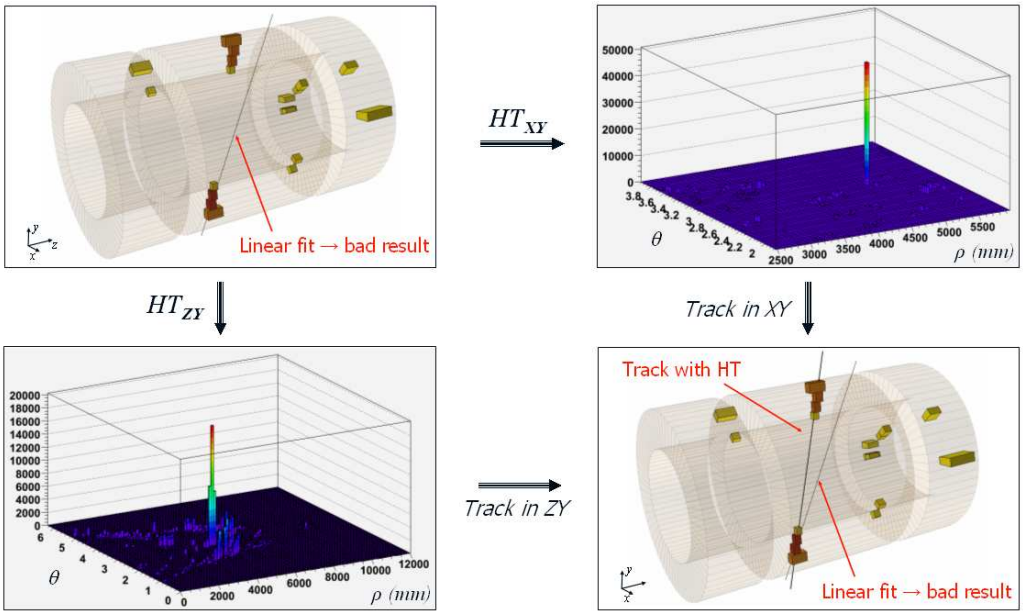

Figure 5: Example of a cosmic ray detection using HT. The fit method returns a wrong result due to the presence of outliers.

comparison as well. One can notice that the fit method produces a wrong result due to the presence of noise cells (outliers) far from the cosmic muon trajectory.

4.2 Signal detection with matched filters

In order to perform the track detection procedure, one should first detect which calorimeter cell has been activated by the cosmic ray. The standard approach is try to estimate the energy deposition in each cell. Then, the decision is given by an energy cut chosen to be a little bit higher than the nominal noise energy (about 100 MeV). However, due to the low signal-to-noise ratio of TileCal for cosmic rays, we have shown that Matched Filters (MF) [19], give better detection efficiency then energy cut method, reducing the noise contamination (outliers) and increasing the track detection efficiency..

The MF approach is based on a hypothesis test. In other words, the detection system has to decide between two possible hypothesis: only the noise is present (called H_0) or both the signal and the additive noise are present (called H_1). The decision rule can be summarized by the Likelihood equation

$$\frac{f_{\mathbf{L}|H_1}(\mathbf{l}|H_1)}{f_{\mathbf{L}|H_0}(\mathbf{l}|H_0)} \underset{H_0}{\overset{H_1}{\gtrless}} \gamma \tag{4.2}$$

where $f_{\mathbf{L}|H_1}(\mathbf{l}|H_1)$ and $f_{\mathbf{L}|H_0}(\mathbf{l}|H_0)$ are the conditional Probability Density Functions (PDFs) for a given outcome $\mathbf{L}$ of N samples, depending on if the hypothesis is either H_1 or H_0, respectively. The constant on the right side of the Equation 4.2 can vary, depending on the costs in deciding between one of the two hypothesis. This equation may be interpreted as following: one decides by H_1 if the probability ratio is higher than γ, otherwise H_0 is chosen.

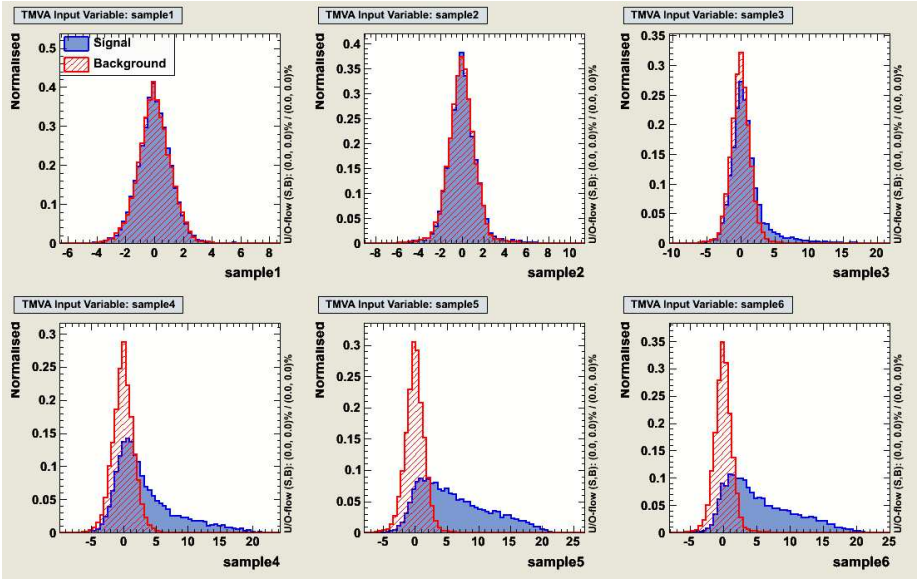

Figure 6: Probability distributions, in ADC counts, of the first six time samples, for both H_1 and H_0 hypotheses.

4.2.1 PDF estimation

During commissioning phase, seven samples of the TileCal time signals are recorded for offline energy reconstruction. Figure 6 shows the probability distribution of the first six samples, in Analog to Digital (ADC) counts, for both hypotheses H_1 and H_0 (Signal and Background respectively). Those distributions were acquired from cosmic ray simulation. In order to store only low signal-to-noise ratio hits, cells with energy deposition higher than 500 MeV were discarded.

As a first PDF estimation approach, the samples will be considered statistically independents. In this way, the PDF will be the productory of individual probability distributions. Even though statistical independence may not be a realistic assumption here, this simple MF approach produces satisfactory detection efficiency results. Further improvements can be done performing some preprocessing techniques, where the samples become either statistically independents or, at least, uncorrelated.

4.2.2 Noise whitening

An important issue to get MF working properly is to make sure that the additive noise is white [19]. The left side of Figure 7 shows the covariance matrix for the TileCal digital noise, where one can see some correlation among neighborhood samples. On the right, the covariance matrix, after some noise whitening transformation [20], is shown. Since the samples of H_0 are uncorrelated in this new base, the estimation of $f_{\mathbf{L}|H_0}(\mathbf{l}|H_0)$ as a productory of individual distributions should give a better approximation.

4.2.3 Preprocessing

The H_1 individual distribution can become uncorrelated, performing some principal component decomposition (Principal Component Analysis - PCA) [21]. PCA projects the distributions in

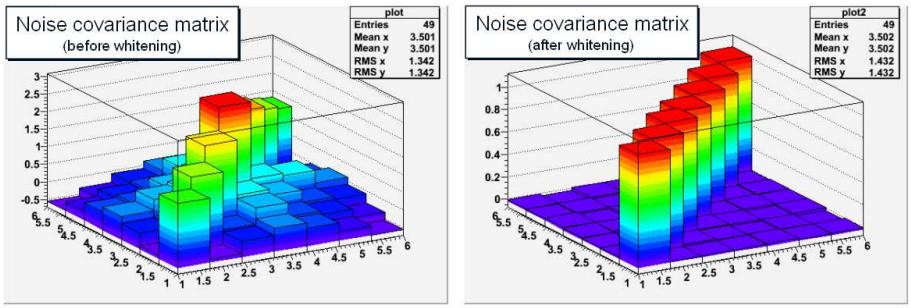

Figure 7: Noise covariance matrix before and after the whitening transformation.

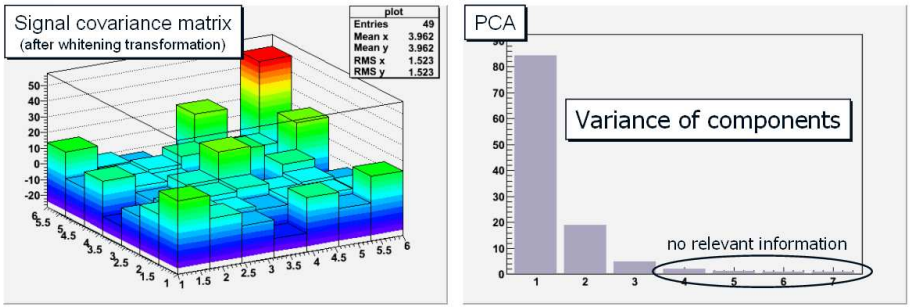

Figure 8: Covariance matrix of H_1. After PCA, signal energy will be concentrated in the three first components.

an orthogonal base, composed by the eigenvectors of the signal covariance matrix. The variance of the new distributions will be the correspondent eigenvalues. Figure 8, left, shows the covariance matrix of H_1 after whitening transformation. On the right, the eigenvalues of this matrix are plotted, sorted by amplitude. One can notice that the signal energy are concentrated on the three first components. Thus, this transformation allow to perform a dimension reduction from 7 to 3 components, without loosing detection efficiency. Besides, since PCA is just a orthonormal transformation (rotation) the noise (H_0) will still be white in this new base.

Since the sample distributions are not gaussian (see Figure 6), PCA and whitening transformations (decorrelation) are not enough to get statistical independence. In order to perform stronger independence decomposition, Independent Component Analysis (ICA) [22] may be applied. ICA is based on the central limit theorem: combinations of nongaussian variables are more gaussian than the original ones. Thus, ICA transformation tries to maximize the nongaussianity of the components. Although methods to measure nongaussianity, like kurtosis and negentropy, have high computational costs, they start to be used more often, thanks to new numeric approximation approaches.

Figure 9 shows the detection efficiency versus the false alarm for different signal detection approaches. All the methods based on matched filters have an efficiency higher than energy cut method. Among the MF methods, the one with ICA preprocessing has the highest efficiency.

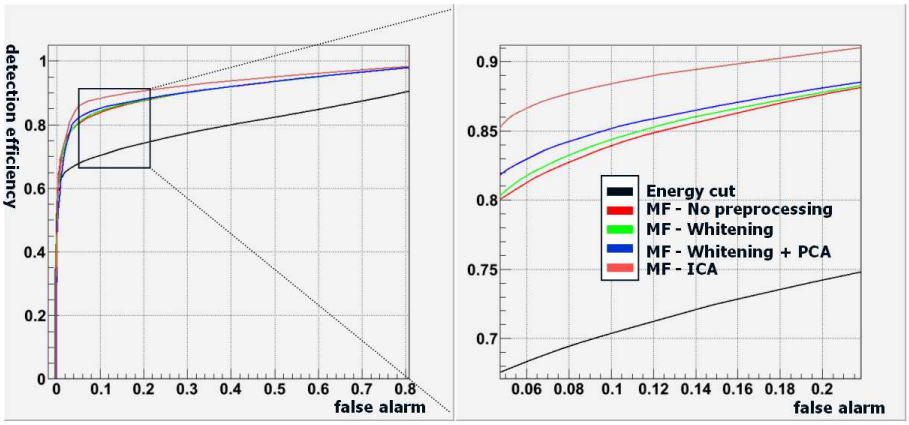

Figure 9: Detection efficiency versus false alarm. All MF approaches give better results than energy cut method.

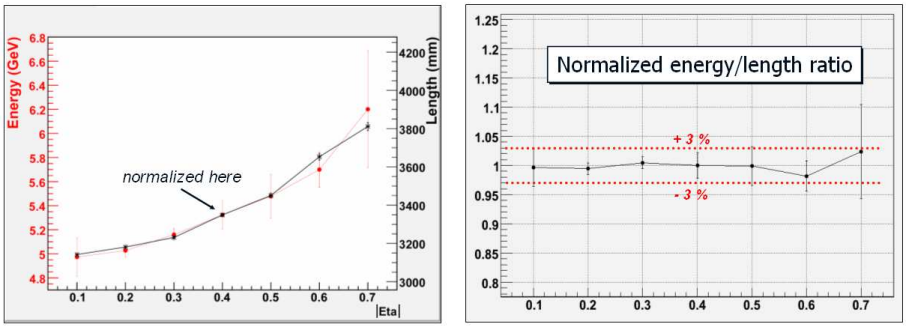

Figure 10: Cosmic muon track length and its correspondent energy deposition as function of $|\eta|$ (left) and normalized energy deposition per unit length in TileCal (right).

5. Experimental results

In order to study the overall uniformity of the TileCal cell energy response, we can compare the measured cosmic muon energy loss from cosmic rays in TileCal to that predicted from the known sampling depth. Figure 10, on the left, shows the cosmic muon track length estimation and its most probable energy deposition value as function of $|\eta|$, for projective events (events crossing the center of the detector) in TileCal. The length, in millimeters, is the mean value for tracks inside the same η region. For each track, the energy deposition was computed by summing the energy of all cells inside a region of interest around the track. The most probable energy deposition corresponds to the peak of a Landau fit over each energy distribution (one for each η region). Due to the low statistics for highest η values, only the first seven TileCal towers were used in this analysis. The normalized energy deposition per unit length (Figure 10, on the right) shows a strong correlation between track length and energy deposition, with a non-uniformity smaller than 3%. One should notice that no cesium calibration had been performed on this data sample, but already at this stage we find that the TileCal cells exhibit a stable energy response.

6. Conclusion

We have presented a combination of Hough Transform and Optimal Filtering techniques in order to detect cosmic rays in highly segmented calorimeters. The MF was used to select activated cells, looking at theirs time digitized samples. We have shown that this approach has higher detection efficiency, comparing to standard energy cut methods. The HT, a well known method to detect line in noisy images, was adapted to detect cosmic ray tracks, using information of activated cells. Analyses of energy deposition per unit length and eta stability tests have shown the good performance of the algorithms.

References

[1] The ATLAS Collaboration, *The ATLAS Experiment at the CERN Large Hadron Collider*, Journal of Instrumentation, JINST 3 S08003, 2008.

[2] https://twiki.cern.ch/twiki/bin/view/Atlas/TileMuonFitter (accessed at December 2008).

[3] G. H. Golub, C. F. Van Loan, *Matrix Computation*, Johns Hopkins Univ. Press, 1984.

[4] P. Hough, *Method and mean for recognizing complex patterns*, United States Patent 3069654, 1962.

[5] H.L.Van Trees. *Detection, Estimation, and Modulation Theory, Part I*, Wiley, 2001.

[6] L. Evans and P. Bryant. *LHC Machine*, Journal of Instrumentation, JINST 3 S08001, 2008.

[7] Eduardo Ros. *ATLAS inner detector*, Nuclear Physics B - Proceedings Supplements, v. 120, pp. 235-238, 2003.

[8] The ATLAS Collaboration. *Calorimeter Performance*, Technical Design Report, CERN/LHCC/96-40, 1997.

[9] P. Perrodo. *The ATLAS liquid argon calorimetry system*, Proceedings of ICHEP, pp. 909-912, 2002.

[10] The ATLAS Collaboration. *Tile Calorimeter*, Technical Design Report, CERN/LHCC/96-42, 1996.

[11] R. Wigmans, *Calorimetry - Energy Measurement in Particle Physics*, Oxford University Press, 2000.

[12] S. Palestini. *The Muon Spectrometer of the ATLAS Experiment*, Nuclear Physics B, v. 125, pp. 337-345, 2003.

[13] S. Falciano. *The ATLAS Level-l and Level-2 trigger*, Nuclear Instruments and Methods in Physics Research A, v. 384, pp. 136-142, 1996.

[14] Gerolf Schlager. *The status and performance of the ATLAS hadronic tile calorimeter*, Nuclear Instruments and Methods in Physics Research A, v. 581, pp. 393-396, 2007.

[15] K.Anderson, J.Pilcher, H.Sanders, F.Tang and R.Teuscher. *Stand-alone Cosmic Ray Trigger Electronics for the ATLAS Tile Calorimeter*. 10th Workshop on Electronics for LHC and future Experiments, Boston, USA, pp. 327-331, 2004.

[16] J. Illingworth. *A survey of the Hough Transform*, Computer Vision, Graphics and Image Processing, v. 44, pp. 87-116, 1988.

[17] M. Ohlsson, C. Peterson. *Track finding with deformable templates*, Computer Physics Communication, v. 71, pp. 77-98, 1992.

[18] J. Illingworth. *The adaptive Hough transform*, Trans. Pattern Analysis and Machine Intelligence, v. 9, n. 5, pp. 690-697, 1987.

[19] K. Sam Shamugan, A.M. Breipohl. *Random Signals - detection, estimation and data analysis*, Wiley, 2001.

[20] H.L.Van Trees. *Detection, Estimation, and Modulation Theory, Part III*, Wiley, 2001.

[21] I. T. Jolliffe. *Principal Component Analysis*, Springer, 2002.

[22] A. Hyvarinen, J. Karhunen. *Independent Component Analysis*, Wiley, 2001.